Mechanics and Mechanical Engineering
Vol. 12, No. 4 (2008) 375–387
© Technical University of Lodz

Aeroflutter Suppression in an FGM Panel with Active Piezoelectric Fibers

Piotr Przybyłowicz
Warsaw University of Technology,
Institute of Machine Design Fundamantals
Narbutta 84, 02–524 Warsaw, Poland

Received (18 November 2008)
Revised (25 November 2008)
Accepted (15 December 2008)

The paper is concerned with the problem of active stabilisation of a flat rectangular plate subject to an aerodynamic load coming from a supersonic air flow tangent to the plate surface. At a suciently high speed, the flow leads to appearance of self–excitated vibration in the system. Such a phenomenon is called the aeroflutter. The main goal of the considerations is to examine to what extent it is possible to prevent the panel from self–excitation and how far it may be suppressed in the non–linear range, if the instability has already occurred. The concept of stabilisation consists in making use of a functionally graded material (FGM) containing an active component piezoceramic PZT. Under electric field, it produces asymmetric longitudinal strain within the cross–section of the plate which generates bending moment opposing the action of non–conservative force induced by the flow. Two simplest control strategies based on differential and proportional feedback are analysed in the paper. The investigation is carried out within the linear range (effect of stabilisation on the critical threshold) as well as non–linear, where the quality of near–critical bifurcating solution is determined in terms of activation of piezoceramic fraction in the FGM structure of the plate.

Keywords: Aeroflutter, self–excitation, bifurcation, functionally graded material, active stabilisation

1. Introduction

A great deal of theoretical work has been done for over than a half century for the problem of flutter of panels exposed to air flow parallel to their surface (Lighthill, [11]), (Kaliski, [9]), (Woroszył, [17]). This phenomenon was, and still is, a research subject for scientists and engineers dealing with aircraft industry and rocket technology as missiles and spacecrafts require very thin coverings. Flutter of various geometrical shapes, under various loading conditions including interactions due to magnetic and thermal fields is still an interesting and complex investigation challenge to be met (Solarz, [15]). Coupled electromagnetic effects accompanying aeroflutter

were studied by Ambartsumian [1] and Kurnik [10] who also thoroughly studied near–critical (non–linear) behaviour of a rectangular plate undergoing self–excited vibration after exceeding critical flow speed. Initially, most of the examination effort was focused on isotropic panels, however advances in material technology quickly forced researchers to consider new structures such as composite laminates (Dixon and Mei, [3]). Recently, the class of anisotropic materials has been enriched with "intelligent" or "smart" structures capable of generating stress and strain controlled according to a special algorithm for a given mechanical purpose (e.g. stabilisation or reduction of vibration amplitude).

Smart composites consist of a matrix material, predominantly polymer, reinforced with fibers partly or entirely possessing some properties making them smart, i.e. controllable by an imput signal (Newnham et al., [12]), (Sporn and Schoencker, [16]). Laminates containing piezoelectric fibers (most often tiny PZT–piezoceramic ones) are able to produce elongation, bending or torsion when exposed to an electric field. Such electromechanical coupling makes the laminates semi, fully adaptive or self–adjusting structures opposing disadvantageous mechanical interactions from surrounding environment or internal phenomena disturbing normal operation of a given system. Smart composites, apart from their load–carrying destination, exhibit enhanced features when compared with their passive counterparts. If needed, they are to dissipate mechanical energy more intensely (Przybyowicz, [14]).

The problem of dynamic stability of plates and shells exposed to conservative forces is permanently changing towards new materials and methods of analysis. Most recently, the studies evolved toward non-homogeneous but different than multi–layered composites Functionally Graded Materials (FGMs), which are a new generation of composite materials with continuous distribution of components within the whole structure. A great deal of theoretical work has been done on thermal stability of FGM panels subject to aerodynamic loads as well. Supersonic flutter characteristics were studied by Prakash and Ganapathi (2004), while non–linear effects in functionally graded panels with von Karman strain–displacement relations were taken into account by Ibrahim et al. (2008). Also smart FGM solutions have appeared in the area of scientists' interest. The problem of active FGMs equipped with piezoelectric materials was examined by He et al. [5], however the applicability of smart elements (piezoelectrical sensors) to active flutter suppression was earlier considered by Dongi et al. [4].

This paper is concerned with active stabilization of a flat rectangular plate under an aerodynamic load by parallel supersonic flow responsible for self-excitation to occur in the system at the critical airflow speed. The plate is made of a functionally graded material containing the active component, which is piezoceramic PZT, and the passive one (fiber reinforced composite). The method of stabilization is based on producing asymmetric longitudinal strain within the cross–section of the plate due to piezoelectric effect, which, consequenltly, generates bending moment to oppose the non–conservative force, and thus stabilize the system. Two simplest approaches toward control are analysed in the paper – one based on differential feedback, the other on proportional.

2. Formulation of the problem

The considered panel is a simply supported plate subject to tangent airflow across the line of supports Fig. 1). The internal structure of the panel constitutes a fiber–reinforced single layer with fibers aligned along the direction of the aerodynamic load. In fact there are two types of fibers in the structure – passive (carbon) and active (piezoceramic). Together, they are equally filled through the thickness, but their individual share varies. Hence, one side of the panel is a fully passive composite, the other – active. Volume fraction of the active piezoceramic fibers varies along the cross–section (Fig. 2.), and this variation is ruled by an exponential function:

$$\eta(z) = \left(\frac{h-2z}{2h}\right)^n \tag{1}$$

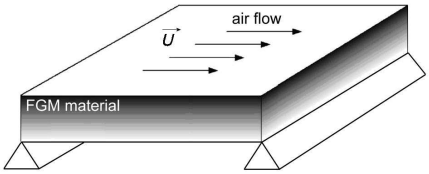

Figure 1 Model of a simply supported FGM panel subject to aerodynamic load

where:

- z – denotes current position through the cross-section,
- h – is the thickness of the panel,
- n – the distribution exponent to be freely assumed in the investigations (e.g. for $n = 1$, the distribution is linear).

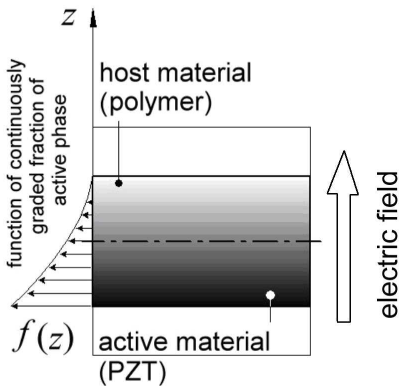

Figure 2 Cross–sectional view to the panel

The function η directly affects the efficient electromechanical coupling constant d_{31}^{T} as well as efficient Young's modulus Y. According to the simple rule, they are as follows:

$$Y(z) = Y_{\mathrm{A}}\eta(z) + Y_{\mathrm{P}}\left[1 - \eta(z)\right] \quad \text{and} \quad d_{31}^{\mathrm{T}}(z) = d_{31(\mathrm{PZT})}^{\mathrm{T}}\eta(z) \tag{2}$$

where the subscripts "$_{\mathrm{A}}$" and "$_{\mathrm{P}}$" refer to the layered passive and active component, respectively.

The governing equation for the panel in its linear formulation has the following form (Kurnik, [10]):

$$\rho\, h\frac{\partial^2 w}{\partial\, t^2} + D\frac{\partial^{\mathbf{4}} w}{\partial\, x^4} + \kappa\frac{p_0}{a_0}\left(\frac{\partial\, w}{\partial\, t} + U\frac{\partial\, w}{\partial\, x}\right) = 0 \tag{3}$$

where the external damping due to interaction with surrounding medium is neglected. Some damping is introduced by the flow itself (the derivative $\partial\, w/\partial\, t$), however the influence of this term was long time ago discussed by Houbolt [6], who suggested its minor effect. Another problem – internal friction in the panel material – is excluded in this analysis. It is an purposely made assumption to expose the effect of the sole active PZT fraction on flutter suppression of the panel. It is, admittedly, known that the presence of internal damping destabilizes such panels, especially at high altitudes (Johns and Parks, [8]).

In equation (3):

w – denotes transverse displacement (vibration) of the panel,
ρ – is the average mass density of the panel,
h – its thickness,
D – rigidity of the panel,
κ – adiabatic constant,
p_0 – pressure of undisturbed air,
a_0 – speed in undisturbed air,
U – speed of the airflow.

The aerodynamic force in (3), see terms inside the parentheses, comes from early considerations by Ashley and Zartarian [2], who developed the so–called piston theory for objects moving through compressible media.

Since the material has continuously varying properties, the stiffness D is in fact the following integral:

$$D = \int\limits_{-\frac{h}{2}}^{\frac{h}{2}} \frac{Y(z)\, z^2\, \mathrm{d}\, z}{1 - v^2(z)} \tag{4}$$

Rewrite, for convenience, the equation of motion into a dimensionless form by introducing following variables:

$$\bar{x} = \frac{x}{l}\ ,\ \ w = \frac{w}{h}\ ,\ \ \bar{t} = \frac{t}{k_t}\ ,\ \ k_t = l^2\sqrt{\frac{\rho\, h}{D}} \tag{5}$$

where l is length of the panel. If so, we obtain:

$$\frac{\partial^2 \bar{w}}{\partial \bar{t}^2} + \frac{\partial^{\mathbf{4}} \bar{w}}{\partial \bar{x}^4} + \gamma \frac{\partial \bar{w}}{\partial \bar{t}} + \upsilon \frac{\partial \bar{w}}{\partial \bar{x}} = 0 \tag{6}$$

where:

$$\gamma = \kappa \frac{p_0}{a_0} \frac{l^2}{\sqrt{\rho\, h\, D}} \quad \text{and} \quad \upsilon = U\, \kappa \frac{p_0}{a_0} \frac{l^3}{D} \tag{7}$$

Introduce now "control" terms, i.e. expressions for the effect brought about by activation of piezoceramic fibers in the panel. According to laws of piezoelectricity [13] the strain–stress relation is:

$$\begin{bmatrix} \varepsilon_1 \\ \varepsilon_2 \\ \varepsilon_3 \\ \varepsilon_4 \\ \varepsilon_5 \\ \varepsilon_6 \end{bmatrix} = \begin{bmatrix} \frac{1}{Y_1} & -\frac{v}{Y_1} & -\frac{v}{Y_3} & 0 & 0 & 0 \\ -\frac{v}{Y_1} & \frac{1}{Y_1} & -\frac{v}{Y_3} & 0 & 0 & 0 \\ -\frac{v}{Y_3} & -\frac{v}{Y_3} & \frac{1}{Y_3} & 0 & 0 & 0 \\ 0 & 0 & 0 & \frac{1}{G_4} & 0 & 0 \\ 0 & 0 & 0 & 0 & \frac{1}{G_4} & 0 \\ 0 & 0 & 0 & 0 & 0 & \frac{1}{G_6} \end{bmatrix} \begin{bmatrix} \sigma_1 \\ \sigma_1 \\ 0 \\ \tau_4 \\ \tau_5 \\ \tau_6 \end{bmatrix} + \begin{bmatrix} 0 & 0 & d_{31} \\ 0 & 0 & d_{31} \\ 0 & 0 & d_{33} \\ 0 & d_{15} & 0 \\ d_{15} & 0 & 0 \\ 0 & 0 & 0 \end{bmatrix} \begin{bmatrix} 0 \\ 0 \\ E \end{bmatrix} \tag{8}$$

where Poisson's ratio has been assumed to have the same value. It is to be remembered that all elements of the matrices depend on the z variable. The longitudinal effect for $\sigma_3 = \sigma_z = 0$ is then:

$$\begin{aligned} \varepsilon_x &= \frac{1}{Y_1}\sigma_x - \frac{v}{Y_3}\sigma_y + d_{31}E \\ \varepsilon_y &= \frac{1}{Y_1}\sigma_y - \frac{v}{Y_3}\sigma_x + d_{31}E \end{aligned} \tag{9}$$

where E denotes electric field applied perpendicularly to the panel (electrodes are on the upper and lower surface) and the main orthotropy directions of PZT coincide with the x and y axes of the plate. Resolving (9) for stresses, one finds:

$$\begin{aligned} \sigma_x &= \frac{Y_1}{1-v^2}\left[\varepsilon_x + v\,\varepsilon_y - d_{31}E(1+v)\right] \\ \sigma_y &= \frac{Y_1}{1-v^2}\left[\varepsilon_y + v\,\varepsilon_x - d_{31}E(1+v)\right] \end{aligned} \tag{10}$$

For cylindrical bending of the plate, the moment produced purely by the piezoceramic fraction is:

$$M_A = -E \int_{-\frac{h}{2}}^{\frac{h}{2}} \frac{Y_1(z)\, d_{31}(z)\, z}{1 - v^2(z)} \mathrm{d}z = -E\,\Delta \tag{11}$$

The electric field Econtrolling the panel, is proportional to the applied voltage U_A:

$$E = \frac{U_A}{h} \tag{12}$$

which, in turn, is proportional to the voltage measured by the sensor attached to the panel at a given position x_s. From sensor considerations related to beams [14], we know that measured voltage is proportional to curvature of the beam (or a plate in cylindrical bending), i.e.:

$$U_S = \frac{Y_{\mathrm{PVDF}}\, d_{31(\mathrm{PVDF})}\, h_s}{\epsilon_0 \epsilon_{\mathrm{PVDF}}}\, \frac{\partial^2 w(x_s,t)}{\partial x^2} \tag{13}$$

where the subscripts "PVDF" refer to the material the sensor is made of (a piezopolymer based on polyvinylidene fluoride), ϵ is dielectric permittivity and h_s – senor thickness. Assume at this moment that the control will be based on a simple feedback coupling with the output signal (from actuator) is directly proportional the first time derivative of the input voltage (from sensor), i.e.:

$$U_A = k_d \dot{U}_S \tag{14}$$

Covering the entire upper and lower surface of the panel with electrodes, we put down an expression for the actuating moment:

$$M_A = -k_d \frac{Y_{\mathrm{PVDF}}\, d_{31(\mathrm{PVDF})}\, h_s}{\epsilon_0 \epsilon_{\mathrm{PVDF}}}\, \frac{\partial^3 w(x_s,t)}{\partial x^2\, \partial t}\, \Delta\, [H(x) - H(x-l)] \tag{15}$$

where H is the Heaviside function. The moment M_A appears in the equation of motion as the second derivative with respect to x. Thus, its final and dimensionless form becomes:

$$\frac{\mathrm{d}\bar{M}_A}{\mathrm{d}\bar{x}} = -k_d \frac{Y_{\mathrm{PVDF}} d_{31(\mathrm{PVDF})}\, h_s}{\epsilon_0 \epsilon_{\mathrm{PVDF}}}\, \frac{\partial^3 \bar{w}(\bar{x}_s bart)}{\partial \bar{x}^2 \partial \bar{t}}\, \frac{\Delta}{l^2 \sqrt{\rho h D}} \left[\frac{\mathrm{d}\delta(\bar{x})}{\mathrm{d}\bar{t}} - \frac{\mathrm{d}\delta(\bar{x}-1)}{\mathrm{d}\bar{t}} \right] \tag{16}$$

where δ is Kronecker's Delta function. Substituting the above expression into the equation of motion, we obtain:

$$\frac{\partial^2 \bar{w}}{\partial \bar{t}^2} + \frac{\partial^4 \bar{w}}{\partial \bar{x}^4} + \gamma \frac{\partial \bar{w}}{\partial \bar{t}} + \upsilon \frac{\partial \bar{w}}{\partial \bar{x}} - c_d \frac{\partial^3 w(x_s,t)}{\partial x^2\, \partial t} \left[\frac{\mathrm{d}\delta(\bar{x})}{\mathrm{d}\,\bar{t}} - \frac{\mathrm{d}\delta(\bar{x}-1)}{\mathrm{d}\,\bar{t}} \right] = 0 \tag{17}$$

where

$$c_d = k_d \frac{Y_{\mathrm{PVDF}}\, d_{31(\mathrm{PVDF})}\, h_s}{\in_0 \in_{\mathrm{PVDF}}}\, \frac{\Delta}{l^2 \sqrt{\rho\, h\, D}} \tag{18}$$

3. Analysis of the flutter suppression efficiency

The main intention now is to find the critical speed of airflow at which the system loses its stability and exhibits self–excited vibration. To achieve this goal, the partial differential equation of motion is transformed into two ordinary differential equations via bimodal Galerkin's discretization based on two simply–supported

beam functions since the flutter-type instability is known to be a two–dimensional definite problem:

$$\bar{w}(\bar{x},\bar{t}) = T_1(\bar{t})\sin\pi\,\bar{x} + T_2(\bar{t})\sin 2\,\pi\,\bar{x} \tag{19}$$

where $T_{1,2}(\bar{t})$ are arbitrary time functions to be determined. Incorporating Galerkin's discretization, one demands:

$$\int_0^1 L\,[\bar{w}(\bar{x},\bar{t})]\;\sin\,n\,\pi\,\bar{x}\,\mathrm{d}\bar{x} = 0 \quad n = 1,\,2 \tag{20}$$

where L represents the operator form of the left hand side of partial differential equation of motion (16). By introducing new variables: $u_1 = T_1$, $u_2 = \dot{T}_1$, $u_3 = T_2$, $u_4 = \dot{T}_2$, we transform the thus generated ordinary differential equations of the second order into a set of four first–order ones. They are as follows:

$$\begin{array}{l}
\dot{u}_1 = u_2 \\
\dot{u}_2 = -\pi^4\,u_1 - (\gamma + 2c_d\pi^3\sin\pi\,x_s)u_2 + \frac{8}{3}\upsilon\,u_3 - 8\,c_d\pi^3\sin 2\pi\,x_s\cdot u_4 \\
\dot{u}_3 = u_4 \\
\dot{u}_4 = -\frac{8}{3}\upsilon\,u_1 - 16\,\pi^4\,u_3 - \gamma\,u_4
\end{array} \tag{21}$$

or in a matrix form:

$$\begin{bmatrix} \dot{u}_1 \\ \dot{u}_2 \\ \dot{u}_3 \\ \dot{u}_4 \end{bmatrix} = \begin{bmatrix} 0 & 1 & 0 & 0 \\ -\pi^4 & \alpha_1 & \frac{8}{3}\upsilon & \alpha_2 \\ 0 & 0 & 0 & 1 \\ -\frac{8}{3}\upsilon & 0 & -16\,\pi^4 & -\gamma \end{bmatrix} \begin{bmatrix} u_1 \\ u_2 \\ u_3 \\ u_4 \end{bmatrix} \tag{22}$$

where:

$$\begin{aligned} \alpha_1 &= -\gamma - 2c_d\pi^3\sin\pi\,x_s \\ \alpha_2 &= -8\,c_d\pi^3\sin 2\pi\,x_s \end{aligned}$$

or implicitly: $\dot{\mathbf{u}} = \mathbf{A}(\upsilon)\mathbf{u}$. It is to be emphasized that the "control" term c_d is not only dependent on the assumed gain k_d in the control system, but it is the dimensionless quantity strongly related to distribution of the active component through the thickness Δ, see (18), and (11) for the explicit expression of Δ. Assume that Poisson's ratio v is poorly changing with z ($v = \mathrm{const}$), which leads, together with (2), to the following integral for Δ:

$$\Delta = \frac{d_{31}}{1-v^2}\int_{-\frac{h}{2}}^{\frac{h}{2}} \{Y_\mathrm{A}\eta(z) + Y_\mathrm{P}\,[1-\eta(z)]\}\,\eta(z)z\,\mathrm{d}z \tag{23}$$

The above integral can be easily computed numerically by simple substitution of given values of the elasticity moduli Y and effective electromechanical coupling constant d_{31}. Let ζ be the ratio between Young's modulus of the active piezoceramic fraction and the passive one:

$$\zeta = \frac{Y_\mathrm{A}}{Y_\mathrm{P}} \tag{24}$$

It is assumed in further analysis that the "hardest" is the active component ($Y_{\mathrm{A}} = 6.25 \cdot 10^{10}$ Pa), while the passive material has only a fraction of its flexural rigidity ranging from 0 to 1.

In Fig. 3, two limit cases when the passive component is (theoretically) rigidless ($\zeta = 0$), and as stiff as the active piezoceramic ($\zeta = 1$). It turns out that discussion on optimal distribution of the active component through the panel thickness is fuitless as the curves for Δ exhibit strongly marked maxima corresponding to some values of n defining the exponential way in which the piezoceramic component vanish along the panel cross–section. It is highly recommended to arrange the FGM structure of the considered panel so that the exponent $n$would just secure those most efficient distributions.

It is possible to find the optimal exponential distributions analytically. Consider now the case when Young's moduli of both components is comparable ($Y_{\mathrm{A}} \approx Y_{\mathrm{P}}$). In that situation integral (23) has the solution:

$$\begin{aligned} \Delta &= \frac{d_{31}\, Y_{\mathrm{A}}}{1-v^2} \int\limits_{-\frac{h}{2}}^{\frac{h}{2}} \eta(z) z \,\mathrm{d}z \\ &= \frac{d_{31}\, Y_{\mathrm{A}}}{1-v^2} \int\limits_{-\frac{h}{2}}^{\frac{h}{2}} \left(\frac{h-2z}{2h}\right)^n z \,\mathrm{d}z \\ &= -\frac{d_{31}\, Y_{\mathrm{A}}\, h^2}{1-v^2} \frac{n}{2(n^2+3n+2)} \end{aligned} \tag{25}$$

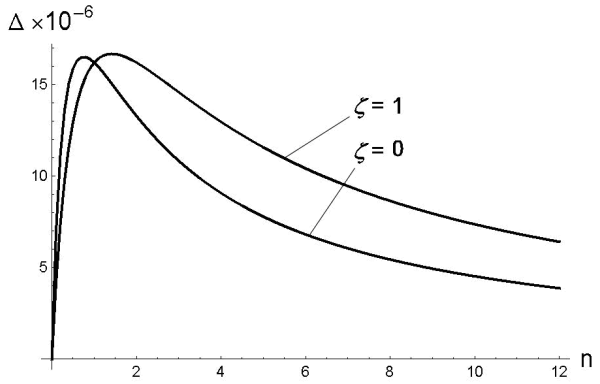

Figure 3 Electromechanical efficiency of the FGM panel vs. exponent of the active component distribution

The maximum value of Δ takes place, when:

$$\frac{\mathrm{d}}{\mathrm{d}\, n}\left(\frac{n}{n^2+3n+2}\right) = 0 \tag{26}$$

which is true for $n = \sqrt{2}$ (see the peak of $\zeta = 1$ curve in Fig. 3). If Young's moduli vary, the problem of determination of the opimal n becomes slightly complicated as it leads to the following integral:

$$\Delta = \frac{d_{31}\, Y_{\mathrm{A}}}{1 - v^2} \int\limits_{-\frac{h}{2}}^{\frac{h}{2}} \left[(1 - \zeta) \left(\frac{h - 2z}{2h} \right)^{2n} - \zeta \left(\frac{h - 2z}{2h} \right)^{n} \right] z \, \mathrm{d}z \tag{27}$$

which yields:

$$\Delta = -\frac{d_{31}\, Y_{\mathrm{A}}\, h^2}{1 - v^2} \frac{n}{2} \left\{ \frac{1 - \zeta}{2n^2 + 3n + 1} + \frac{1}{n^2 + 3n + 2} \right\} \tag{28}$$

The derivative of (28) with respect to n gives a rational function whose numerator is to be equaled with zero for extremum. This gives the following polynomial of the fourth degree:

$$2\, n^4 (1 + \zeta) + 4n^3 (2 - \zeta) + 7n(1 - 2\zeta) - 4n(1 + \zeta) - 2(2 - \zeta) = 0 \tag{29}$$

It has four roots, but their analytical form is too far complex to be explicitly given in thsese consideration. A better method is illustrating the solution to (29) graphically for ζ varying within the assumed interval, see Fig. 4.

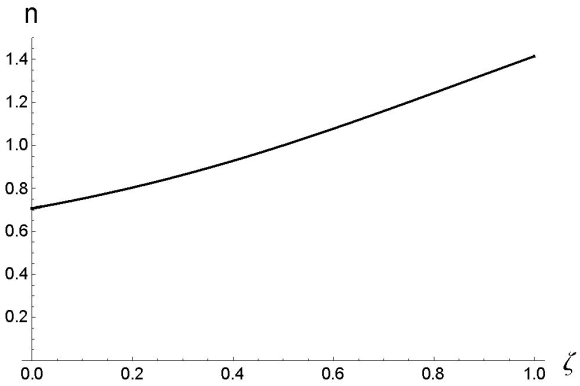

Figure 4 The most effective exponents of the active fraction distribution in function of the elasticity ratio between Young's moduli of the active and passive components

It is only to be noted that (29) becomes easily solvable again for the other limit case, i.e. when $\zeta = 0$. In such circumstances, $n = 1/\sqrt{2}$.

4. Simulation results

Having determined the most effective volume distributions of the active component in the FGM panel, investigate now the effect of flutter suppression by the proposed

method based on the strategy incorporating velocity feedback in the control system. For this purpose, find first the critical airflow speed at which the panel loses its stability. This can be achieved by tracing eigenvalues of the matrix $\mathbf{A}$ of the discretized equations of motion. The eigenvalues come from the following eigenproblem:

$$\{\mathbf{A}(\upsilon) - r\,\mathbf{I}\}\ \mathbf{q} = \mathbf{0} \tag{30}$$

where r is the eigenvalue to be searched for and $\mathbf{q}$ – corresponding eigenvector. The eigenvalue having the greatest real part decides about stability of the system. It will be denoted by r_1.

In Fig. 5. some trajectories of the decisive eigenvalue are shown for growin Mach number of the airflow. Left picture of Fig. 5 clearly indicates the critical air speed responsible for the loss of stability as the real part of r_1 becomes positive. The right picture shows trajectories of r_1 on the complex plane, where the imaginary part of r_1 as it croses the imaginary axis depicts the initial flutter frequency.

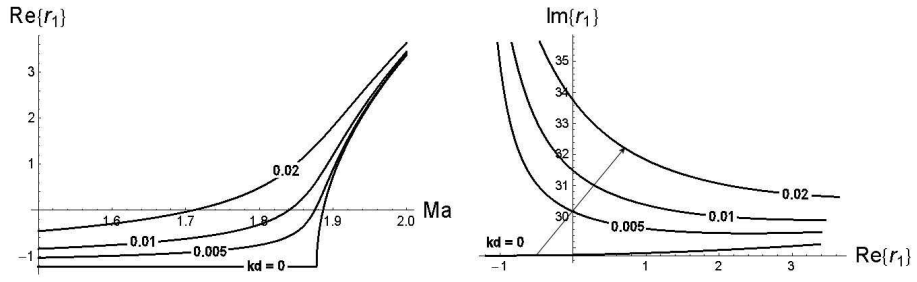

Figure 5 Trajectories of the decisive eigenvalue for differential feedback control

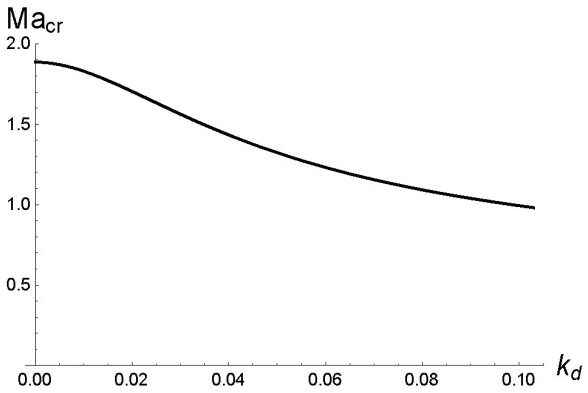

Figure 6 Critical Mach number for the control based on differential feedback

Fig. 5 presents several curves corresponding to a few of assumed gains in the control system for the most efficient functional distribution of the active component (here $n = \sqrt{2}$ for comparable Young's moduli of both components of the FGM). Unfortunately, the results reveal disadvantageous effects of the applied stabilisation method. The real part $\mathrm{Re}\{r_1\}$ for non–zero gains k_d intersects the zero threshold for continuously lower flow speed with an increase in the gain. The trajectories on the right picture in Fig. 5 shift rightwards. A destabilizing effect is obvious. It is more conveniently shown in Fig. 6, where the critical Mach number versus the applied gain factor is presented in its dropping shape. The reason for that surprising and disappointing effect is due to the fact that the velocity feedback introduces damping-like terms to the equation of motion, which are known to destabilize panels exposed to aerodynamic loads (Johns and Parks, 1960). Probably, the generation of counter–bending moment in the FGM structure does not compensate the introduced damping.

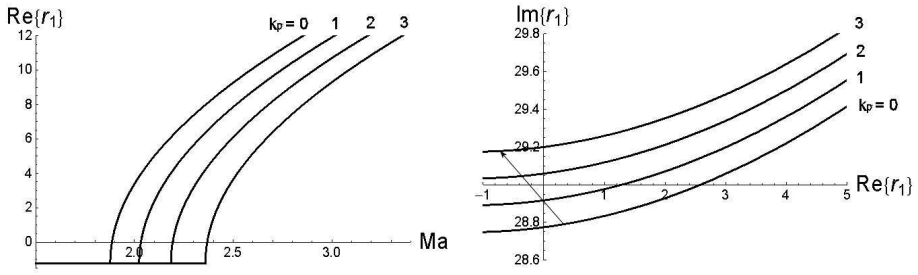

Figure 7 Trajectories of the decisive eigenvalue for proportional feedback

In the light of such a result, another – yet equally simple – control strategy has been proposed to reach the goal. This time the electric field inducing bending moment within the entire FGM structure is to be directly proportional to the measured voltage (related to current curvature of the panel).

$$U_A = k_p U_S \tag{31}$$

This is a "P" control enhancing rigidity of the analysed system. Since it affect terms in the equation of motion related to stiffness, the Galerkin discretization must be carried out again. With the new variables u_1 employed, it gives:

$$\begin{bmatrix} \dot{u}_1 \\ \dot{u}_2 \\ \dot{u}_3 \\ \dot{u}_4 \end{bmatrix} = \begin{bmatrix} 0 & 1 & 0 & 0 \\ \alpha_3 & -\gamma & \alpha_4 & 0 \\ 0 & 0 & 0 & 1 \\ -\frac{8}{3}\upsilon & 0 & -16\,\pi^4 & -\gamma \end{bmatrix} \begin{bmatrix} u_1 \\ u_2 \\ u_3 \\ u_4 \end{bmatrix} \tag{32}$$

where:

$$\begin{aligned} \alpha_3 &= -\pi^4 - 2c_p\pi^3 \sin \pi\, x_s \\ \alpha_4 &= 8\left(\frac{\upsilon}{3} - c_p\pi^3 \sin 2\pi\, x_s\right) \end{aligned}$$

The subsequent analysis proceeds as previously. For easy investigation, the eigenvalues are found once more and illustrated. The results are shown in Fig. 7.

Now, the suppression effect is noticeable. Stronger gains k_p make the decisive eigenvalue trajectories move leftwards (right diagram in Fig. 7) which means that the real part of r_1 intersects the critical threshold for greater speeds of the airflow, see Fig. 8.

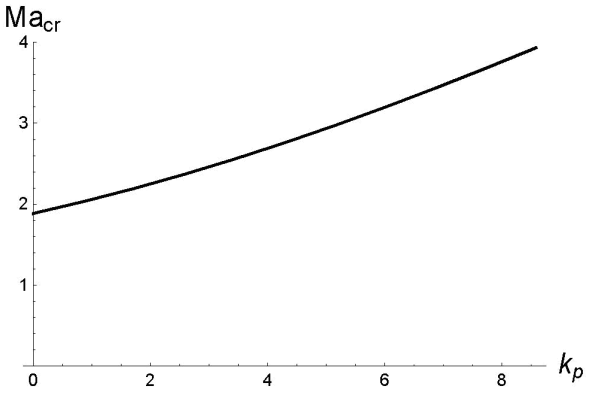

Figure 8 Critical Mach number for the control based on proportional feedback

The suppression effect has been finally achieved. It is yet to be remembered that such a strategy may shortly lead to dielectric breakdowns within the active piezoceramic fibers if the applied gains k_p reach excessively high levels.

5. Concluding remarks

The main goal of the paper was to analyse the efficiency of a method for aeroflutter suppression of a flat FGM panel containing an active piezoceramic component in form of tiny fibers reinforcing the composite structure of the panel. Two control strategies have been analysed in detail. It occurred that differential feedback leads to disadvantageous results as the critical threshold (airflow speed at which self–excitated flutter–type vibration occurs) drops for such a strategy. Most probably, the capability of the approach does not compensate the additional damping–like effect introduced by the velocity coupling between the input and output signal. Fortunately, the proportional coupling turned out to be fully effective, endangered however by electric malfunction due to possible dielectric breakdown if excessive coefficients of that proportionality were assumed.

An interesting achievement of the study was presentation of a method for estimating the best exponential distributions of the active component through the panel thickness that yield the most pronounced electromechanical effect contributing to flutter suppression in the panel. The method uniquely indicates the optimal distributions provided that the electric field is directly applied through the panel thickness by electrodes attached to both surfaces of the panel. Some results are derived and proved in a pure analytical manner.

References

[1] **Ambartsumian, S.A.**: Magnetoelasticity of Thin Plates and Shells, *Applied Mechanics Review*, 35(1), 1–5, **1982**.

[2] **Ashley, H. and Zartarian, G.**: Piston Theory – a New Aerodynamic Tool for the Aeroelastician, Journal of the Aeronautical Science, 23(10), 1109-1118, **1956**.

[3] **Dixon and I.R., Mei, C.**: Finite Element Analysis of Large-Amplitude Panel Flutter of Thin Laminates, *Journal of American Institute of Aeronautics and Astronautics*, 31(3), 701-707, **1993**.

[4] **Dongi, F., Dinkler, D. and Kroplin, B.**: Active Panel Suppression Using Self–Sensing Piezoactuators, *Journal of American Institute of Aeronautics and Astronautics*, 34(5), 1224-1230, **1996**.

[5] **He X.Q., Ng, T.Y., Sivashanker and S. and Liew K.M.**: Active Control of FGM Plates with Integrated Piezoelectric Sensors and Actuators, *International Journal of Solids and Structures*, 38, 1641-1655, **2001**.

[6] **Houbolt, J.C.**: A Study of Several Aerothermoelatic Problems of Aircraft Structures in High Speed Flight, Doctoral Thesis, ETH Zurich, **1958**.

[7] **Ibrahim, H.H., Tawfik, M. and Al–Ajmi, M.**: 2007, Non-linear Panel Flutter for Temperature–Dependent Functionally Graded Material Panels, *Computational Mechanics*, 41(2), 325-334, **2007**.

[8] **Johns, D.J. and Parks, P.C.**: Effect of Structural Damping on Panel Flutter: Stability of Two-Dimensional Simply-Supported Panels Using Linear Piston Theory, *Aircraft Engineering and Aerospace Technology*, 32(**??**), 304-308, **1960**.

[9] **Kaliski, S.**: Drgania i fale, PWN Warszawa, **1966**.

[10] **Kurnik, W.**: Bifurkacje dywergentne i oscylacyjne, Wydawnictwa Naukowo Techniczne, Warszawa, **1997**.

[11] **Lighthill, M.J.**: Oscillating Airfolis At High Mach Number, Journal of the Aeronautical Science, 20(5), 402-406, **1953**.

[12] **Newnham, R.E., Bowen, K.A., Klicker, K.A. and Cross, L.E.**: Composite Piezoelectric Transducers, *Material Engineering*, 2, 93-106, **1980**.

[13] **Nye, J.F.**: Physical Properties of Crystals, Oxford: Clarendon, **1985**.

[14] **Przybyłowicz, P.M.**: Piezoelectric Vibration Control of Rotating Structures, Prace Naukowe Politechniki Warszawskiej, Mechanika, z. 197, Oficyna Wydawnicza PW, **2002**.

[15] **Solarz, L.**: Aero-Magneto-Flutter of a Plane Duct of Finite Length, *Proceedings of Vibration Problems*, 7, 347-361, **1966**.

[16] **Sporn, D. and Schoencker, A.**: Composites with Piezoelectric Thin Fibers – First Evidence of Piezoelectric Behaviour, *Materials Research Innovations*, 2, 303-308, **1999** .

[17] **Woroszył, S.**: Coupled Local and Integral Flutter of a Cylindrical Shell in Linearized Flow, *Proceedings of Vibration Problems*, 7, 67-83, **1966**.